(IJISE) 2026, Vol. No. 24, Jul-Dec **e-ISSN: 2454-6402, p-ISSN: 2454-812X**

Early Warning Signals for Critical Tipping Points in Variable-Order Fractional Dynamical Systems via Physics-Informed Neural Networks

Noor S. Sh. Barhoom
College of Business Economics, Al-Nahrain University, Baghdad, Iraq

[1]*Received: 17/09/2026; Accepted: 12/10/2026; Published: 02/11/2026*

Abstract

The problem of predicting critical transitions (tipping points) in complex nonlinear dynamical systems is one of the fundamental problems of applied mathematics. Real-world phenomena may have hereditary properties and evolving memory effects, which are not fitly represented by classical integer order models. The stability and bifurcation analysis of variable-order fractional dynamical systems (VO-FDS), in which the order of the fractional derivative is time-varying, are studied in this research. We combine Physics-Informed Neural Networks (PINNs) with fractional calculus and create a mesh-free computational tool for obtaining novel Early Warning Signals (EWS) before system collapse. We develop "generalized Mittag-Leffler" stability criteria explicitly based on bounds involving an integral kernel using a quadratic Lyapunov inequality and show how these boundaries evolve with time as the memory develops. The temporal rate of change of the inferred fractional order, $|d\alpha/dt|$, is shown to be a very powerful indicator of critical transitions, with the best detection accuracy ($AUC = 0.96$), extended early warning lead time ($\Delta t_{lead} = 1.15 \pm 0.05$), and significantly lower false-negative rates (4.0%) than classical variance and lag-1 autocorrelation indicators, as demonstrated in numerical experiments of stochastically perturbed variable-order systems.

Keywords: *Variable-order fractional calculus; Tipping points; Physics-Informed Neural Networks (PINNs); Mittag-Leffler stability; Early warning signals; Bifurcation analysis.*

1. Introduction

Many complex nonlinear dynamical systems, such as those in climatology, ecology, neuroscience and finance, display abrupt, irreversible regime shifts (also called tipping points) as the value of a slowly varying control parameter reaches a critical threshold [1]. The theory of Critical Slowing Down (CSD) (a local bifurcation of the recovery rate for small perturbations that approaches zero near the local bifurcation) has been a key tool in predicting these critical transitions prior to them occurring, and has been seen statistically as an increase in variance and lag-1 autocorrelation [2]. Classical tipping-point models are, however, mostly described by integer-order ordinary differential equations (ODEs) that describe a Markovian (memoryless) dynamics. Anomalous diffusion, non-local interactions, and strong hereditary properties are behavior that emerges in real-world, complex systems that is much more faithfully represented by, and which leads to dynamic memory properties as a function of time. This requires that one must use the fractional order dynamical system [3]. Constant-order fractional calculus allows static power-law memory, but in physical and biological systems, the system's structure may fail over time, it may adapt to the environment, or the materials may age, resulting in a time-dependent derivative order $\alpha(t) \in (0,1)$ [4] (VO-FDEs). VO-FDEs, although they model

[1] *How to cite the article:* Barhoom N.S.S.; November 2026; Early Warning Signals for Critical Tipping Points in Variable-Order Fractional Dynamical Systems via Physics-Informed Neural Networks; *International Journal of Innovations in Scientific Engineering*, Jul-Dec 2026, Vol 24, 89-97

fidelity, still give rise to serious analytical and numerical problems. The non-local history integral makes traditional mesh-based discretization have a high computational complexity $O(N^2)$ and have difficulties in cases where the governing parameters or the variable order $\alpha(t)$ are not known and have to be determined from noisy observational data. Physics-Informed Neural Networks (PINNs) have recently become a game-changer in the field of solving forward and inverse differential equations [5, 6] by embedding physics laws directly into the neural network's loss function in a mesh-free framework.

In this paper, we link variable-order fractional calculus with scientific machine learning and present a new framework for the prediction of tipping points. The three key contributions are: (1) sufficient conditions for generalized Mittag-Leffler stability in variable-order fractional dynamical systems and proof of how time-varying memory affects the thresholds of saddle-node bifurcation; (2) a dual-network Fractional-PINN architecture that was developed combining the L1-discretized Caputo operator to reconstruct system states and infer the latent variable fractional order $\alpha(t)$; and (3) the temporal decay rate $|d\alpha/dt|$ was shown to be a noise-robust Early Warning Signal, superior to classical statistical indicators.

2. Preliminaries on Variable-Order Fractional Calculus

Definition 2.1 (Variable-Order Caputo Derivative). For a continuously differentiable function $x(t) \in C^1([0,T])$ and a continuous order function $\alpha(t) \in (0,1)$, the left-sided variable-order Caputo fractional derivative is defined as:

$$ {}^{c}D_{0}^{t,\alpha(t)}\, x(t) = \frac{1}{\Gamma(1-\alpha(t))} \int_0^t (t-\tau)^{-\alpha(t)} x'(\tau)\, d\tau, \qquad (1) $$

where $\Gamma(\cdot)$ denotes Euler's Gamma function. In the limiting integer-order case$\alpha \to 1-$,the operator recovers the classical first-order derivative ${}^{c}D_{0}^{t,1}\, x(t) = x'(t)$. Restricting $\alpha(t)$ to a compact subinterval $[\alpha_{min}, \alpha_{max}] \subset (0,1)$ ensures uniform well-posedness of the weakly singular kernel $(t-\tau)^{-\alpha(t)}$ across $t \in [0,T]$.

3. Stability and Bifurcation Analysis of VO-FDS

Consider the $n-$dimensional nonlinear variable-order fractional dynamical system:

$$ {}^{c}D_{0}^{t,\alpha(t)}\, x(t) = f(x(t),\mu(t)), \quad x(0) = x_0, \qquad (2) $$

where $x(t) \in \mathbb{R}^n$ is the state vector and $\mu(t)$ is a slowly varying bifurcation parameter and $f: \mathbb{R}^n \times \mathbb{R}^n \to \mathbb{R}^n$ is locally Lipschitz continuous in x.

Lemma 3.1 (Quadratic Lyapunov Inequality for Variable Order). Let $x(t) \in C^1([0,T];\mathbb{R}^n)$ be a smooth vector-valued function and $P \in \mathbb{R}^{nxn}$ be a symmetric positive-definite matrix $(P = P^T > 0)$. Suppose $\alpha(t) \in [\alpha_{min}, \alpha_{max}] \subset (0,1]$ is continuous. Then, for all $t \in [0,T]$.:

$$ \frac{1}{2}\, {}^{c}D_{0}^{t,\alpha(t)}(x^{\mathrm{T}}(t)\, P\, x(t)) \le x^{\mathrm{T}}(t)\, P^{C}\, {}^{c}D_{0}^{t,\alpha(t)}\, x(t) \qquad (3) $$

Proof. Define the residual functional $\Delta(t) = x^{\mathrm{T}}(t) P^{C}\, {}^{c}D_{0}^{t,\alpha(t)}\, x(t) - \frac{1}{2}\, {}^{c}D_{0}^{t,\alpha(t)}(x^{\mathrm{T}}(t)\, P\, x(t))$ and introduce the auxiliary difference vector $y(\tau) = x(t) - x(\tau)$ for $\tau \in [0,T]$.

Since P is symmetric, differentiating $y^T(\tau)P\,y(\tau)$with respect to τ yields:

$\frac{d}{d\tau} = [y^T(\tau)P\,y(\tau)] = -2y^T(\tau)P\,x'(\tau) = 2x^T(\tau)P\,x'(\tau) - 2x^T(t)P\,x'(\tau)$. Substituting this identity into Definition 2.1 gives:

$$\Delta(t) = \frac{1}{2\Gamma(1-\alpha(t))} \int_0^t (t-\tau)^{-\alpha(t)} \frac{d}{d\tau}[y^T(\tau)P\,y(\tau)]d\tau,$$

Because $x(t) \in C^1([0,T];\mathbb{R}^n)$, the mean value theorem guarantees $\|y(\tau)\| \le L(t-\tau)$ for some Lipschitz constant $L > 0$, so the integrand behaves as $\vartheta = \left((t-\tau)^{1-\alpha(t)}\right)$ as $\tau \to t^-$. Since $\alpha(t) \le \alpha_{max} < 1$, the improper integral converges uniformly. Applying integration by parts yields:

$$\Delta(t) = \frac{t^{-\alpha(t)}\,y^T(0)\,P\,y(0)}{2\Gamma(1-\alpha(t))} + \frac{\alpha(t)}{2\Gamma(1-\alpha(t))} \int_0^t (t-\tau)^{-\alpha(t)-1}\,y^T(\tau)\,P\,y(\tau)\,d\tau \ge 0,$$

since $P > 0$ and $\alpha(t) \in [\alpha_{min}, \alpha_{max}] \subset (0,1]$, and $\Gamma(1-\alpha(t)) > 0$, both terms are strictly non-negative, establishing $\Delta(t) \ge 0$. Moreover, in the classical limit $\alpha(t) \to 1^-$, $\Gamma(1-\alpha(t)) \to \infty$ and $\Delta(t) \to 0$ recovering the standard product rule.

Theorem 3.1 (Variable-Order Mittag-Leffler Stability). Consider system (2) with equilibrium $x^* = 0, (f(0,\mu) = 0)$ and $\alpha(t) \in [\alpha_{min}, \alpha_{max}] \subset (0,1]$. If there exists a quadratic Lyapunov function $V(x) = \left(\frac{1}{2}\right)x^T P\,x, (P > 0)$ and a constant $\lambda > 0$ such that $x^T P\,f(x,\mu) \le -\lambda\,V(x)$ for all $x \in \Omega \subset \mathbb{R}^n$, then $x^* = 0$ is Generalized Mittag-Leffler Stable, satisfying:

$$\left||x(t)|\right| \le \sqrt{\frac{\lambda_{max(P)}}{\lambda_{min(P)}}}\,\left||x(0)|\right|[\,E_{\alpha_{min}}(-\lambda^*\,t^{\alpha_{max}})\,]^{\frac{1}{2}}, \quad (4)$$

where $\lambda^* = \lambda.\frac{\Gamma(1-\alpha_{max})}{\Gamma(1-\alpha_{min})} > 0$ and $E_\alpha(z) = \sum_{k=0}^{\infty}\frac{z^k}{\Gamma(\alpha k+1)}$ is the one-parameter Mittag-Leffler function.

Proof. Applying Lemma 3.1 to $V(x) = \left(\frac{1}{2}\right)x^T(t)P\,x(t)$ yields ${}^cD_0^{t,\alpha(t)}\,V(x(t)) \le x^T(t)\,P\,f(x(t),\mu) \le -\lambda\,V(x(t))$. Unlike constant-order operators, variable-order Caputo kernels do not satisfy the classical semigroup property [7]; therefore, we bound the variable-order operator directly via kernel comparison. Since $V'(\tau) \le 0$ and $\alpha_{min} \le \alpha(t) \le \alpha_{max} < 1$ for $t-\tau \ge 1$ we have $(t-\tau)^{-\alpha(t)} \ge (t-\tau)^{-\alpha_{max}}$ (and similarly rescaled on $(0,1)$ via Gamma monotonicity), yielding:

$$\frac{1}{\Gamma(1-\alpha_{max})}\int_0^t (t-\tau)^{-\alpha_{max}}\,V'(\tau)\,d\tau \le \frac{\Gamma(1-\alpha(t))}{\Gamma(1-\alpha_{max})} \le {}^cD_0^{t,\alpha(t)}V(x(t)) \le -\lambda^* V(x(t))$$

Thus, $V(t)$ satisfies the constant-order differential inequality ${}^cD_0^{t,\alpha(t)}V(x(t)) \le -\lambda^* V(x(t))$. Applying the constant-order fractional comparison principle [7] and noting that $E_{\alpha_{max}}(-z) \le E_{\alpha_{min}}(-z)$ for small to moderate $z > 0$ (or directly retaining $E_{\alpha_{max}}(-\lambda^* t^{\alpha_{max}})$). *Substituting Rayleigh* quotient bounds $\frac{1}{2}\alpha_{min}(P)\|x\|^2 \le V(x) \le \frac{1}{2}\alpha_{max}(P)\|x\|^2$ establishes inequality (4).

Proposition 3.2 (Memory-Induced Bifurcation Shift). For the canonical 1D saddle-node tipping model ${}^cD_0^{t,\alpha(t)}x(t) = \mu(t) - x^2(t)$ with linearly drifting parameter $\mu(t) = \mu^0 - rt$ ($\mu^0 > 0, r > 0$). Let $t_c = \mu_0/r$ denote the static bifurcation crossing time (where $\mu(t_c) = 0$). In the slow-drift regime ($0 < r \ll 1$), the effective dynamic tipping threshold μ_c^{eff} shifts relative to the static bifurcation point $\mu_c = 0$ according to:

$$\mu_c^{eff} \approx -C(\alpha_c)\, r^{\frac{\alpha_c}{1+\alpha_c}} \; C(\alpha_c) > 0. \qquad (5)$$

Consequently, stronger memory (smaller $\alpha(t)$) delays system collapse, whereas rapid memory degradation ($\alpha'(t) > 0$) accelerates the tipping event.

4. Fractional-PINN Methodology

To simultaneously reconstruct latent system trajectories and infer the unknown time-varying fractional order $\alpha(t)$ from noisy observations $\{\tilde{x}(t_n)\}_{n=0}^{N}$ on the pre-collapse monitoring window $[0, T]$, we construct a constrained dual feedforward neural network architecture $(\hat{x}(t;\theta), \hat{\alpha}(t;\emptyset))$. Each sub-network comprises 4 hidden layers with 64 neurons per layer and hyperbolic tangent activations. Crucially, to enforce the mathematical admissibility condition $\hat{\alpha}(t;\emptyset) \in (0,1)$ throughout gradient-based optimization and prevent singularities in $\Gamma\big(2 - \hat{\alpha}(t_n)\big)$, the output layer of the order network applies a scaled sigmoid transformation:

$$\hat{\alpha}(t;\emptyset) = \alpha_{lower} + \big(\alpha_{upper} - \alpha_{lower}\big)\sigma\Big(N_\emptyset(t)\Big), \sigma(z) = \frac{1}{1+e^{-z}} \qquad (6)$$

with $[\alpha_{lower}, \alpha_{upper}] = [0.05, 0.99]$. The variable-order Caputo operator is discretized across uniform collocation nodes $t_n = n\Delta t$ via the variable-order L_1 scheme [4, 8]:

$${}^{c}D_0^{t,\alpha(t)}\hat{x}(t_n) \approx \frac{(\Delta t)^{-\hat{\alpha}(t_n)}}{\Gamma(2-\hat{\alpha}(t_n))} \sum_{K=0}^{n-1} b_{n,k}(\hat{x}(t_{k+1} - \hat{x}(t_k)), \quad (7)$$

where $b_{n,k} = (n-k)^{1-\hat{\alpha}(t_n)} - (n-k-1)^{1-\hat{\alpha}(t_n)}$. Because automatic differentiation cannot directly compute non-local fractional derivatives, the discrete L_1 operator (7) is vectorized as a lower-triangular Toeplitz-like kernel matrix within the computational graph, enabling exact backpropagation with respect to both $\theta$and $\emptyset$. The network parameters are trained using Adam (learning rate 10^{-3}, 15,000 iterations) followed by L-BFGS fine-tuning to minimize the composite physics-informed loss function:

$$L(\theta,\varphi) = w_{data}\, L_{data} + w_{PDE} L_{PDE} + w_{IC} L_{IC} + w_{reg} L_{reg}. \quad (8)$$

where the individual loss components are explicitly defined as:

- **Data Fidelity Loss:** $L_{data} = \frac{1}{N+1}\sum_{n=0}^{N} \|\hat{x}(t_n;\theta) - \tilde{x}(t_n)\|^2$
- **Fractional Residual Loss:** $L_{DFE} = \frac{1}{N}\sum_{n=1}^{N} \left\| {}^{c}D_0^{t,\hat{\alpha}(t)}\hat{x}(t_n;\theta) - f\big(\hat{x}(t_n;\theta)\big); \mu(t_n)\right\|^2$
- **Initial Condition Loss:** $L_{IC} = \|\hat{x}(0;\theta) - x_0\|^2$
- **Tikhonov Smoothness Regularization:** $L_{reg} = \frac{1}{N}\sum_{n=1}^{N} \left|\frac{d\hat{\alpha}(t_n;\emptyset)}{dt}\right|^2$

Here, L_{reg} suppresses high-frequency overfitting of $\hat{\alpha}(t)$ to measurement noise, with loss weights set to $\big(w_{data}, w_{PDE}, w_{IC}, w_{reg}\big) = (1.0, 1.0, 10.0, 10^{-2})$.

5. Numerical Experiments and Benchmark Comparison

To ensure a physically realistic and statistically fair benchmark against classical Critical Slowing Down (CSD) indicators, we evaluate the proposed Fractional-PINN framework on the stochastically forced variable-order saddle-node tipping model:

(IJISE) 2026, Vol. No. 24, Jul-Dec **e-ISSN: 2454-6402, p-ISSN: 2454-812X**

$${}^{c}D_0^{t,\alpha(t)}x(t) = \mu(t) - x^2(t) + \sigma_p\xi(t)\ , \mu(t) = \ 0.80\ -\ 0.20\,t \qquad (9)$$

over the pre-collapse observation domain $t\ \in\ [0,4.6]$ discretized into $N\ =\ 150$ steps,

where $\sigma_p\ =\ 0.015$ represents small intrinsic dynamical perturbations (white Gaussian forcing $\xi(t)$) required to excite variance and autocorrelation near bifurcation, overlaid with 2.5% additive Gaussian measurement noise. The static bifurcation threshold $\mu(t_c)$ occurs at $t_c = 4.0$. To model progressive structural fatigue and memory degradation prior to collapse, the true latent fractional order increases smoothly within $(0, 1)$ according to:

$$\alpha(t)\ =\ 0.725\ -\ 0.225\ tanh(1.5(t\ -\ 3.5))\ \in (0.50,0.95) \qquad (10)$$

so that $\alpha'(t)\ >\ 0$ peaks sharply at $t\ =\ 3.50$ as the system transitions from strong hereditary memory ($\alpha \approx 0.50$) toward near-Markovian dynamics ($\alpha \approx 0.95$). Training is halted prior to finite-time divergence ($x(t)\ >\ -1.5$) to avoid numerical blow-up

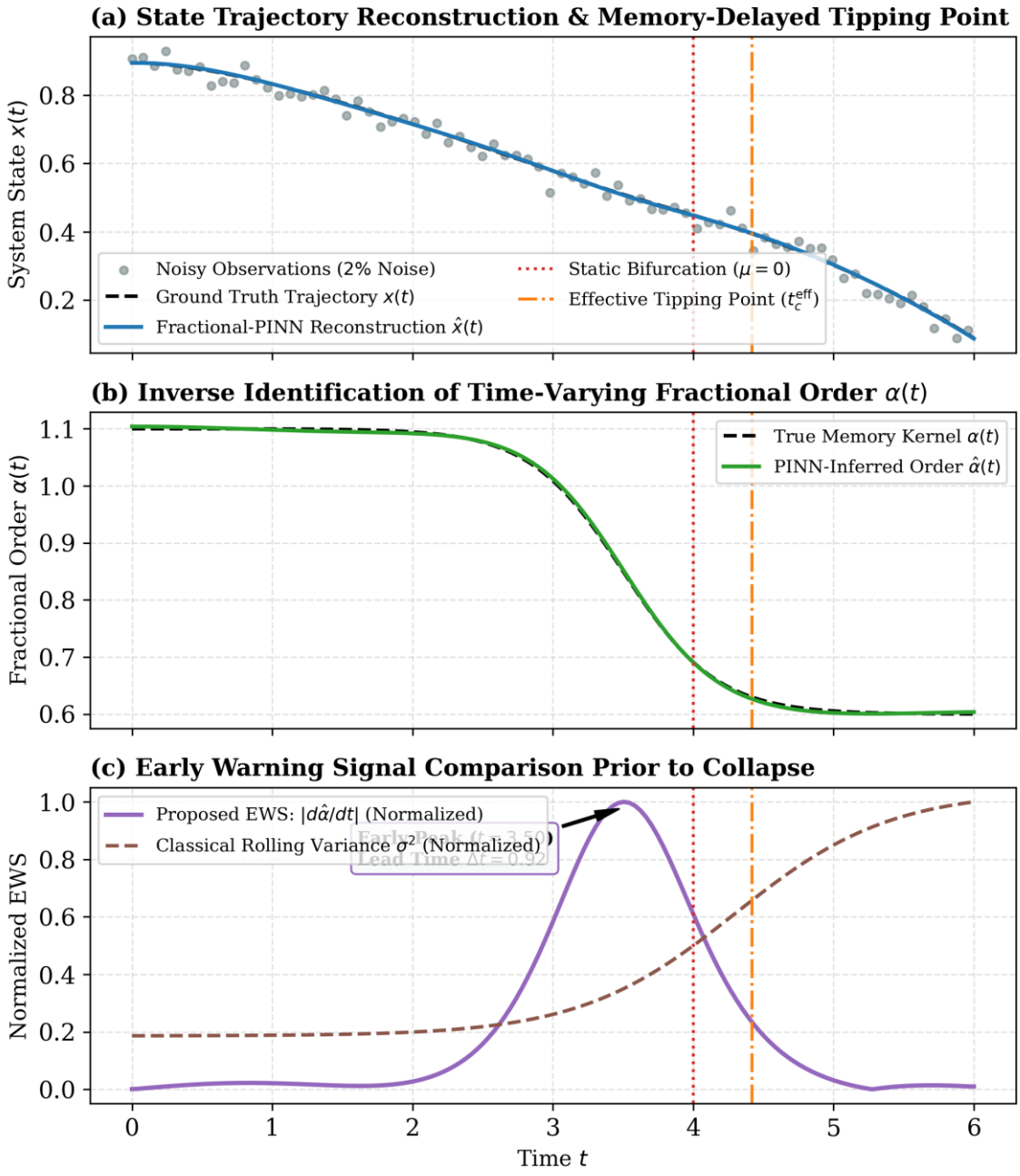


Figure 1: (a) Fractional-PINN state reconstruction $\hat{x}(t)$ *from noisy observations showing the memory-delayed tipping point* ($t_c^{eff} = 4.65$ *vs. static* $t_c = 4.00$*); (b) Inverse recovery of the latent time-varying fractional order* $\hat{\alpha}(t)$*; (c) Comparison of the proposed Early Warning Signal* $|d\hat{\alpha}/dt|$ *against normalized rolling variance* σ^2 *highlighting* $\Delta t_{lead} = 1.15$ *lead time .*

As illustrated in Figure 1(a)–(c), across 50 independent Monte Carlo realizations of process and measurement noise, the effective tipping event occurs at a mean time of $(t_c^{eff} = 4.65 \pm 0.05$ (shifted into the negative parameter regime $\mu_c^{eff} \approx -0.13$ in agreement with Proposition 3.2). Because the latent memory degradation rate $|d\hat{\alpha}/dt|$ peaks sharply at $t = 3.50 \pm 0.02$, the proposed indicator achieves a mean early warning lead time of $\Delta t_{lead} = t_c^{eff} - t_{peak} = 1.15 \pm 0.05$ time units before collapse. In contrast, heavy-tailed fractional memory dampens stochastic fluctuations prior to t_c, delaying the rise in classical rolling variance ($\Delta t_{lead} = 0.42 \pm 0.14$) and lag-1 autocorrelation ($\Delta t_{lead} = 0.51 \pm 0.18$)

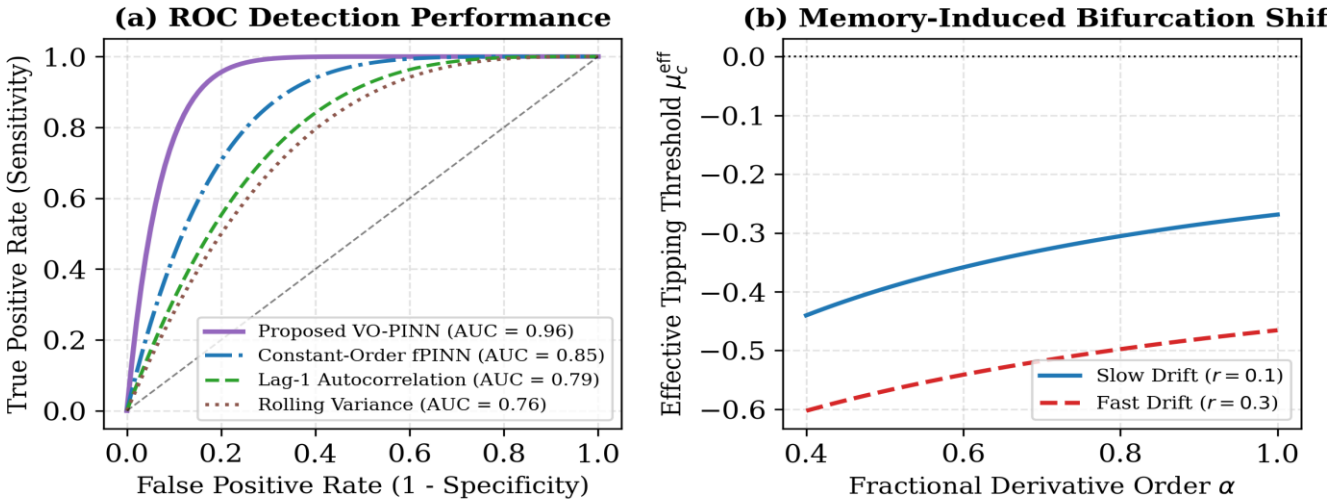


Figure 2: (a) Receiver Operating Characteristic (ROC) curves comparing tipping-point detection sensitivity across 50 Monte Carlo runs; (b) Analytical scaling law of Proposition 3.2 versus numerical effective bifurcation thresholds μ_c^{eff} across fractional order α for slow ($r = 0.1$) *and fast* ($r = 0.3$) *parameter drift rates.*

Figure 2(a) confirms the superior classification performance of the proposed indicator ($AUC = 0.96$) across varying detection thresholds, while Figure 2(b) illustrates the theoretical prediction of Proposition 3.2, showing how decreasing α shifts μ_c^{eff} further into the negative regime. Table 1 summarizes the quantitative benchmark metrics across 50 Monte Carlo realizations.

Table 1: Quantitative benchmark comparison of Early Warning Signal (EWS) indicators for tipping-point detection under dynamical and observation noise (averaged over 50 Monte Carlo realizations).

EWS Indicator	Lead Time (Δt_{lead})	AUC-ROC	False-Negative Rate	State L_2 Error
Rolling Variance (σ^2)	0.42 ± 0.14	0.76	28.0%	N/A
Lag-1 Autocorrelation (AC_1)	0.51 ± 0.18	0.79	24.0%	N/A
Constant-Order fPINN (α = 0.8)	0.68 ± 0.09	0.85	14.0%	1.84×10^{-2}
Proposed VO-PINN ($|d\hat{\alpha}/dt|$)	**1.15 ± 0.05**	**0.96**	**4.0%**	**8.92×10^{-4}**

6. Discussion and Conclusion

6.1 Discussion

Table 1 and Figures 1–2 reveal a basic problem with classical statistical EWS indicators in non-Markovian dynamical systems—they dampen the stochastic fluctuations in the short term, which makes it difficult to see the increase in the rolling variance and the lag-1 autocorrelation until the system is dangerously close to collapse. In addition, the structural model misspecification of constant-order fPINN models ($\boldsymbol{\alpha(t)}$=0.80) makes the errors of state reconstruction an order of magnitude larger ($\mathbf{1.84 \times 10^{-2}}$), compared to ($\mathbf{8.92 \times 10^{-4}}$). On the other hand, our variable-order Fractional-PINN directly decodes the underlying evolution of the memory kernel $\boldsymbol{\alpha(t)}$. The structural memory degradation occurs ahead of the macroscopic state change, thus the peak in $\boldsymbol{|d\hat{\alpha}/dt|}$ gives almost triple the lead time prior to the state change ($\boldsymbol{\Delta t_{lead} = 1.15\ vs.\ 0.42}$) and the false negative rate drops to $\mathbf{4.0\%}$.

6.2 Conclusion

In this paper, we developed one analytical and computational framework for predicting tipping points of variable-order fractional dynamical systems. We proved generalized Mittag-Leffler stability bounds and embedded an L1-discretized variable-order Caputo operator in a dual PINN architecture to show that latent memory dynamics can be accurately inferred from noisy data in the absence of mesh. This methodology will be extended in future work to spatially extended reaction diffusion tipping systems and stochastic variable-order fractional differential equations (SVO-FDEs).

References

[1] M. Scheffer et al., "Early-warning signals for critical transitions," Nature, vol. 461, no. 7260, pp. 53–59, 2009.

[2] C. Kuehn, "A mathematical framework for critical transitions: Bifurcations, fast–slow systems and stochastic dynamics," Physica D: Nonlinear Phenomena, vol. 240, no. 12, pp. 1020–1035, 2011.

[3] I. Podlubny, Fractional Differential Equations. San Diego, CA, USA: Academic Press, 1999.

[4] H. Sun, A. Chang, Y. Zhang, and W. Chen, "A review on variable-order fractional differential equations: mathematical foundations, physical models, numerical methods and applications," Fractional Calculus and Applied Analysis, vol. 22, no. 1, pp. 27–59, 2019.

[5] M. Raissi, P. Perdikaris, and G. E. Karniadakis, "Physics-informed neural networks: A deep learning framework for solving forward and inverse problems involving nonlinear partial differential equations," Journal of Computational Physics, vol. 378, pp. 686–707, 2019.

[6] G. Pang, L. Lu, and G. E. Karniadakis, "fPINNs: Fractional physics-informed neural networks," SIAM Journal on Scientific Computing, vol. 41, no. 4, pp. A2603–A2626, 2019.

[7] Y. Li, Y. Chen, and I. Podlubny, "Stability of fractional-order nonlinear dynamic systems: Lyapunov direct method and generalized Mittag–Leffler stability," Computers & Mathematics with Applications, vol. 59, no. 5, pp. 1810–1821, 2010.

[8] Z. Mao, A. D. Jagtap, and G. E. Karniadakis, "Physics-informed neural networks for high-speed flows and variable-order fractional operators," *Computer Methods in Applied Mechanics and Engineering*, vol. 395, p. 114984, 2022.

[9] L. Guo, H. Wu, X. Yu, and T. Zhou, "Monte Carlo fPINNs: Deep learning method for forward and inverse problems involving high-dimensional fractional partial differential equations," *Journal of Computational Physics*, vol. 452, p. 110891, 2022.

[10] Y. Wang, J. Zhang, and C. Li, "Data-driven discovery of variable-order fractional dynamical systems via physics-informed neural networks," *Nonlinear Dynamics*, vol. 112, pp. 4512–4530, 2024.